

## Supplementary Information:

### **2,2':6',2''-Terpyridine-functionalized redox-responsive hydrogels as a platform for multi responsive amphiphilic polymer membranes**

Katrin Schöllera,†, Claudio Toncellia,†, Juliette Experton<sup>a</sup>, Susanne Widmer<sup>a</sup>, Daniel Rentsch<sup>b</sup>, Aliaksei Vetushka<sup>c</sup>, Colin Martin<sup>d</sup>, Manfred Heuberger<sup>a</sup>, Catherine. E. Housecroft,<sup>d</sup> Edwin C. Constable<sup>d</sup>, Luciano F. Boesel<sup>a,\*</sup>, Lukas J. Scherer<sup>a</sup>

<sup>a</sup> Empa, Swiss Federal Laboratories for Materials Science and Technology, Lerchenfeldstrasse 5, 9014 St. Gallen, Switzerland

<sup>b</sup> Empa, Swiss Federal Laboratories for Materials Science and Technology, Überlandstrasse 129, 8600 Dübendorf, Switzerland

<sup>c</sup> Laboratory of Nanostructures and Nanomaterials, Institute of Physics AS CR, Cukrovarnicka 10, 162 00 Prague 6, Czech Republic

<sup>d</sup> Department of Chemistry, University of Basel, Spitalstrasse 51, 4056 Basel, Switzerland

E-mail: Luciano.Boesel@empa.ch

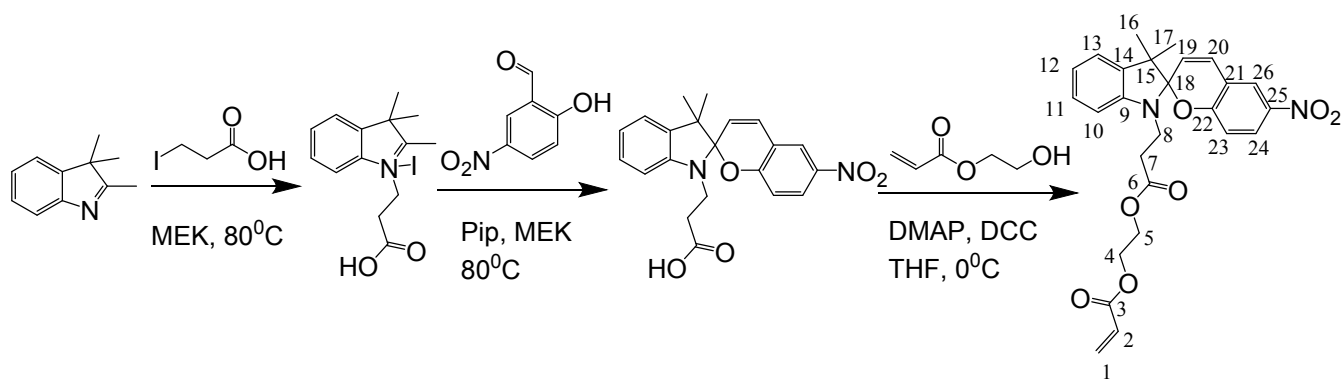
## NMR Experimental

$^1\text{H}$  and  $^{13}\text{C}$  NMR spectra were obtained at 298 K on a Bruker Avance 400 (at 400.1 and 100.6 MHz) or Bruker Avance III-500 (at 500 and 126 MHz) spectrometer (Bruker Biospin AG, Fällanden, Switzerland). The 1D  $^1\text{H}$  and  $^{13}\text{C}$  NMR spectra and the  $^1\text{H}$ - $^1\text{H}$ , and  $^1\text{H}$ - $^{13}\text{C}$  2D correlation experiments were performed at 298 K using a 5 mm BBI inverse probe equipped with z-gradient. All spectra were recorded with the Bruker standard pulse programs and parameter sets and the  $^1\text{H}/^{13}\text{C}$  chemical shifts were referenced internally using the resonance signals of  $\text{CD}_3\text{OD}$  at 3.31/49.0 ppm or of  $\text{CDCl}_3$  at 7.26/77.0 ppm, respectively. Coupling constants  $J$  are reported in Hz and for  $^1\text{H}$  NMR data coupling patterns are described as s = singlet, d = doublet, t = triplet, q = quartet, m = multiplet, br = broad. For  $^{13}\text{C}$  NMR data s = quaternary carbon, d = CH, t =  $\text{CH}_2$ , q =  $\text{CH}_3$  group and w = weak HMBC correlation.

## Synthesis of SP and TP1 monomers

### Synthesis of SP:

Spirobenzopyran SP was synthesized as reported in literature with an overall yield of 36 %<sup>1,2</sup>.



**Scheme S-1.** Synthesis of SP by coupling of an acrylic to the spirobenzopyran moiety

<sup>1</sup>H NMR (CDCl<sub>3</sub>, 400.1 MHz): δ 8.01 (dd, J = 8.6+2.7, 1H, H-24); 7.99 (m, 1H, H-26); 7.20 (m, 1H, H-11); 7.08 (m, 1H, H-13); 6.92 (d, J = 10.4, 1H, H-20); 6.88 (m, 1H, H-12); 6.74 (d, J = 8.6, 1H, H-23); 6.61 (m, 1H, H-10); 6.39 (dd, J = 17.3+1.4, 1H, H-1a); 6.09 (dd, J = 17.3+10.4, 1H, H-2); 5.86 (d, J = 10.4, 1H, H-19); 5.85 (dd, J = 10.4+1.4, 1H, H-1b); 4.31 (m, 2H, H-4); 4.24 (m, 2H, H-5); 3.64 (m, 1H, H-8a); 3.52 (m, 1H, H-8b); 2.71 (m, 1H, H-7a); 2.6 (m, 1H, H-7b); 1.26 (s, 3H, H-16); 1.14 (s, 3H, H-17).  
<sup>13</sup>C NMR (CDCl<sub>3</sub>, 100.6 MHz): δ 171.6 (s, C-6); 165.8 (s, C-3); 159.3 (s, C-22); 146.3 (s, C-9); 141.1 (s, C-25); 136.0 (s, C-14); 131.5 (t, C-1); 128.4 (d, C-20); 127.9 (d, C-2); 127.8 (d, C-11); 125.7 (d, C-24); 122.7 (d, C-26); 122.0 (d, C-19); 121.9 (d, C-13); 119.9 (d, C-12); 118.6 (s, C-21); 115.3 (d, C-23); 106.8 (d, C-10); 106.7 (s, C-18); 62.2 (t, C-5); 62.0 (t, C-4); 52.9 (s, C-15); 39.1 (t, C-8); 33.4 (t, C-7); 25.8 (q, C-17); 19.8 (q, C-16).

<sup>1</sup>H-<sup>13</sup>C HMBC correlations: H-1a → C-(2w, 3); H-1b → C-(3); H-2 → C-(3w); H-4 → C-(3, 5); H-5 → C-(4, 6); H-7a → C-(6, 8); H-7b → C-(6, 8); H-8a → C-(6, 7, 9, 18); H-8b → C-(6, 7w, 9, 18w); H-10 → C-(12, 14); H-11 → C-(9, 13); H-12 → C-(10, 13, 14); H-13 → C-(9, 11, 12w, 15); H-16 → C-(14, 15, 17, 18); H-17 → C-(14, 15, 16, 18); H-19 → C-(18, 21); H-20 → C-(18, 21, 22, 26); H-23 → C-(21, 22w, 25); H-24 → C-(22, 25w, 26); H-26 → C-(20, 22, 24, 25w). Note: We observed no <sup>3</sup>J correlation from H-19 to C-15, probably due to an unfavorable (small) bond angle of H-19/C-19/C-18/C-15.

<sup>1</sup>H-<sup>1</sup>H DQF-COSY correlations: H-1a → H-(1b, 2); H-1b → H-(1a, 2); H-2 → H-(2); H-4 → H-(5); H-5 → H-(4); H-7a → H-(7b, 8a, 8b); H-7b → H-(7a, 8a, 8b); H-8a → H-(7a, 7b, 8b); H-8b → H-(7a, 7b, 8a); H-10 → H-(11); H-11 → H-(10, 12); H-12 → H-(11, 13); H-13 → H-(12); H-19 → H-(20); H-20 → H-(19); H-23 → H-(24); H-24 → H-(23).

IR (cm<sup>-1</sup>): 1733.0 (s), 1622.4 (m), 1483.0 (m), 1407.6 (m), 1248.2 (s), 1164.0 (s), 1023.5 (m), 964.0 (m), 911.7 (m), 837.0 (m), 797.7 (m).

UV (nm): 585, 620

MS (pos., m/z): 469.16

Elem. Anal.: calcd: [C] 71.78%, [H] 5.16%, [N] 5.98%, obsd: [C] 68.11%, [H] 5.29%, [N] 5.39%.

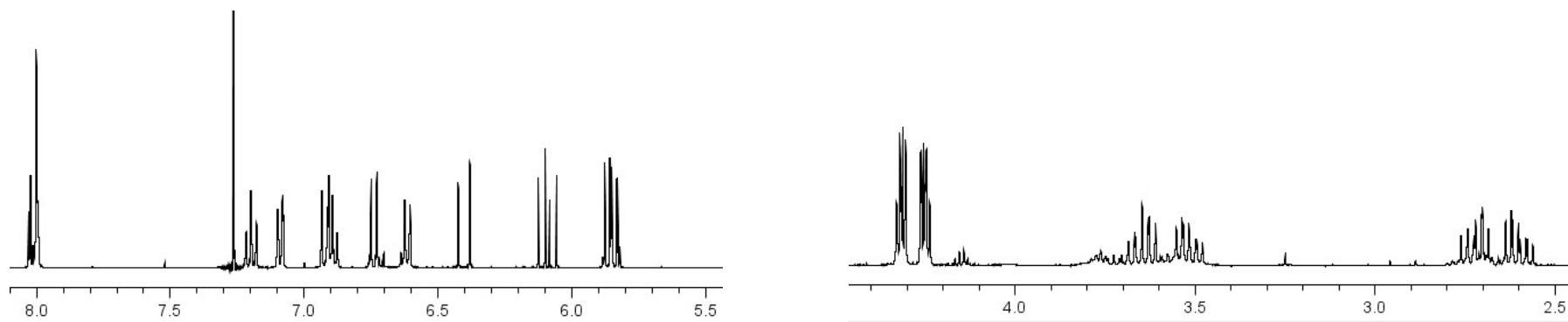


**Figure S-1a.** Regions of interest of  $^1\text{H}$  NMR spectra of SP monomer (in  $\text{CDCl}_3$ )

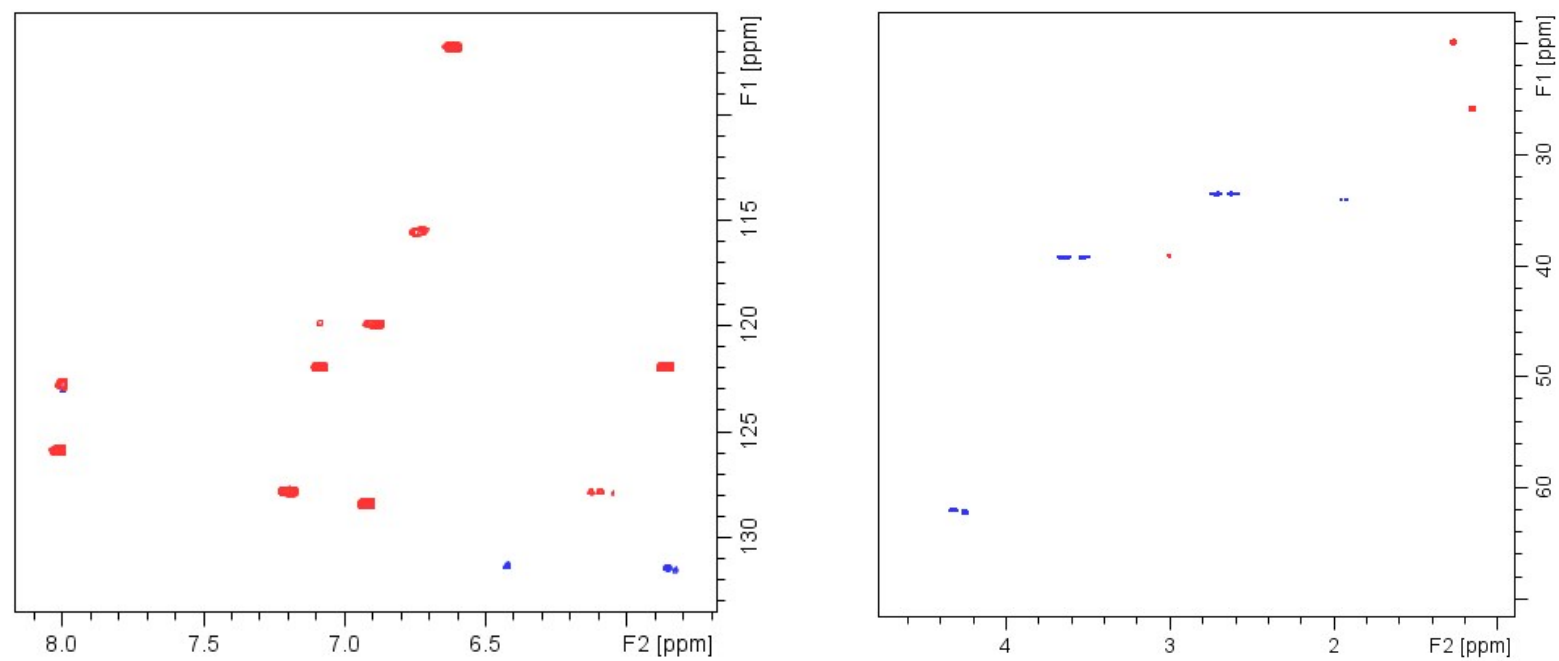


**Figure S-1b.** Regions of interest of  $^1\text{H}$ - $^{13}\text{C}$  HSQC NMR spectra of SP monomer (in  $\text{CDCl}_3$ )

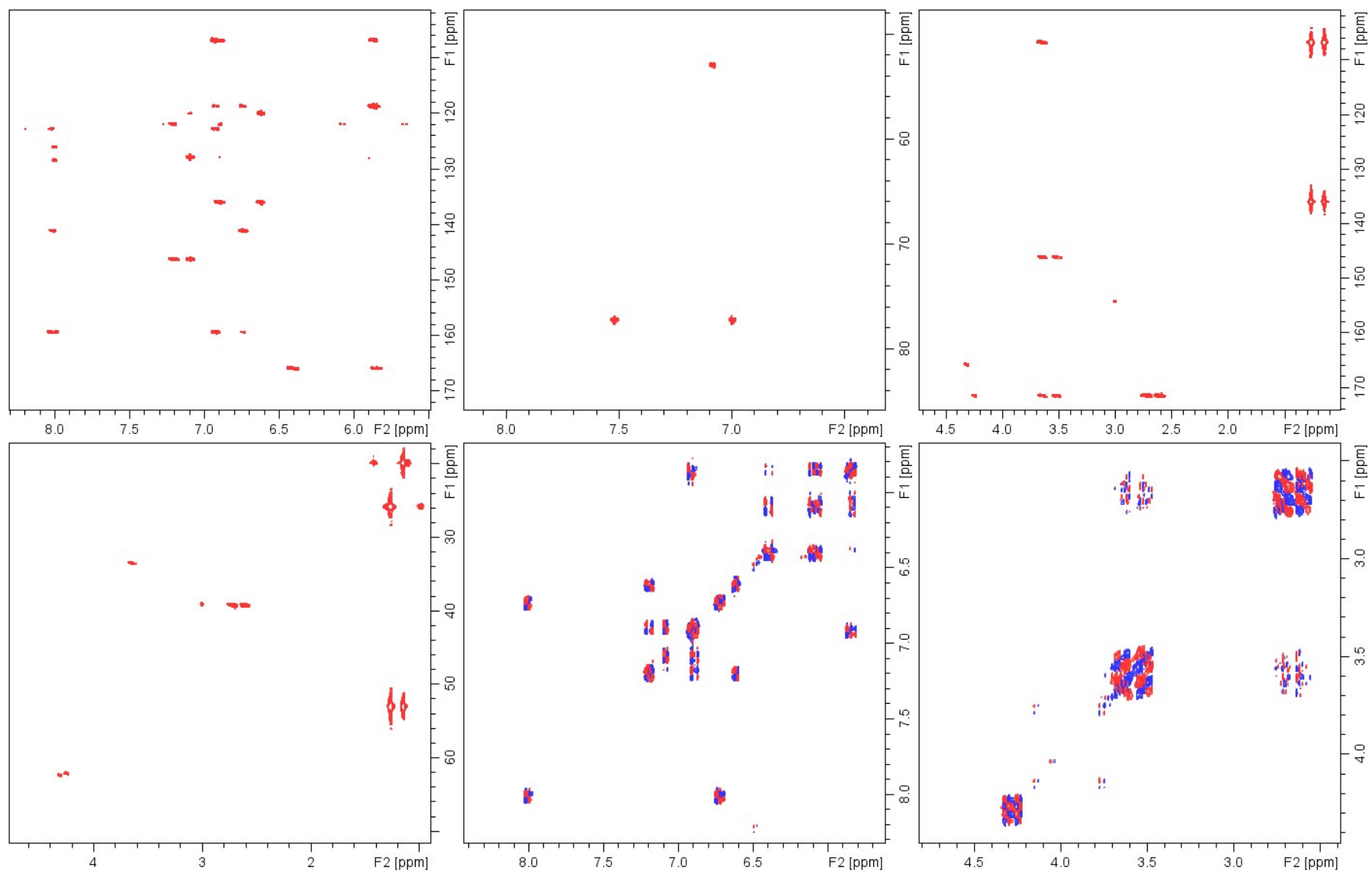
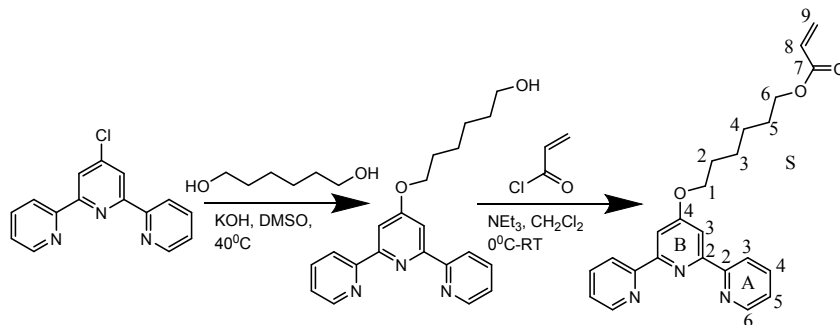


**Figure S-1c.** Regions of interest of  $^1\text{H}$ - $^{13}\text{C}$  HMBC and  $^1\text{H}$ - $^1\text{H}$  DQF-COSY NMR spectra of SP monomer (in  $\text{CDCl}_3$ )

## Synthesis of TP1

Terpyridine 1 (TP1) synthesized according to literature (49 % yield)<sup>3</sup>.



**Scheme S-2.** Synthesis of TP1 via coupling of hexane-1,6-diol with terpyridine followed by addition of an acrylic monomer.

<sup>1</sup>H NMR (CDCl<sub>3</sub>, 400.1 MHz): δ 8.72 (ddd, J = 4.8+1.8+0.8, 2H, H-A6); 8.66 (ddd, J = 7.8+1.1+0.8, 2H, H-A3); 8.06 (s, 2H, H-B3); 7.89 (ddd, J = 7.8+7.5+1.8, 2H, H-A4); 7.37 (ddd, J = 7.5+4.8+1.1, 2H, H-A5); 6.40 (dd, J = 17.3+1.5, 1H, H-S9a); 6.12 (dd, J = 17.3+10.4, 1H, H-S8); 5.80 (dd, J = 10.4+1.5, 1H, H-S9b); 4.27 (t, J = 6.4, 2H, H-S1); 4.18 (t, J = 6.7, 2H, H-S6); 1.88 (m, 2H, H-S2); 1.72 (m, 2H, H-S5); 1.55 (m, 2H, H-S3); 1.48 (m, 2H, H-S4).

<sup>13</sup>C NMR (CDCl<sub>3</sub>, 100.6 MHz): δ 167.5 (s, C-B4); 166.3 (s, C-S7); 156.3 (s, C-B2); 155.5 (s, C-A2); 148.5 (d, C-A6); 137.5 (d, C-A4); 130.5 (t, C-S9); 128.7 (d, C-S8); 124.0 (d, C-A5); 121.7 (d, C-A3); 107.9 (d, C-B3); 68.3 (t, C-S1); 64.5 (t, C-S6); 28.9 (t, C-S2); 28.5 (t, C-S5); 20.7 (t, C-S4); 20.7 (t, C-S3).

<sup>1</sup>H-<sup>13</sup>C HMBC correlations: H-A3 → C-(A5, B2); H-A4 → C-(A2, A6); H-A5 → C-(A3, A6); H-A6 → C-(A2, A4, A5); H-B3 → C-(A2, B3, B4); H-S1 → C-(B4, S2, S3); H-S2 → C-(S1, S3, S4); H-S3 → C-(S1, S2, S4, S5); H-S4 → C-(S2, S3, S5, S6); H-S5 → C-(S3, S4, S6); H-S6 → C-(S4, S5, S7); H-S8 → C-(S7, S9); H-S9a → C-(S7, S8); H-S9b → C-(S7, S8).

<sup>1</sup>H-<sup>1</sup>H DQF-COSY correlations: H-A3 → H-(A4); H-A4 → H-(A3, A5); H-A5 → H-(A4, A6); H-A6 → H-(A5); H-S1 → H-(S2); H-S2 → H-(S1, S3); H-S3 → H-(S2, S4); H-S4 → H-(S3, S5); H-S5 → H-(S4, S6); H-S6 → H-(S5); H-S8 → H-(S9a, S9b); H-S9a → H-(S8, S9b); H-S9b → H-(S8, S9a).

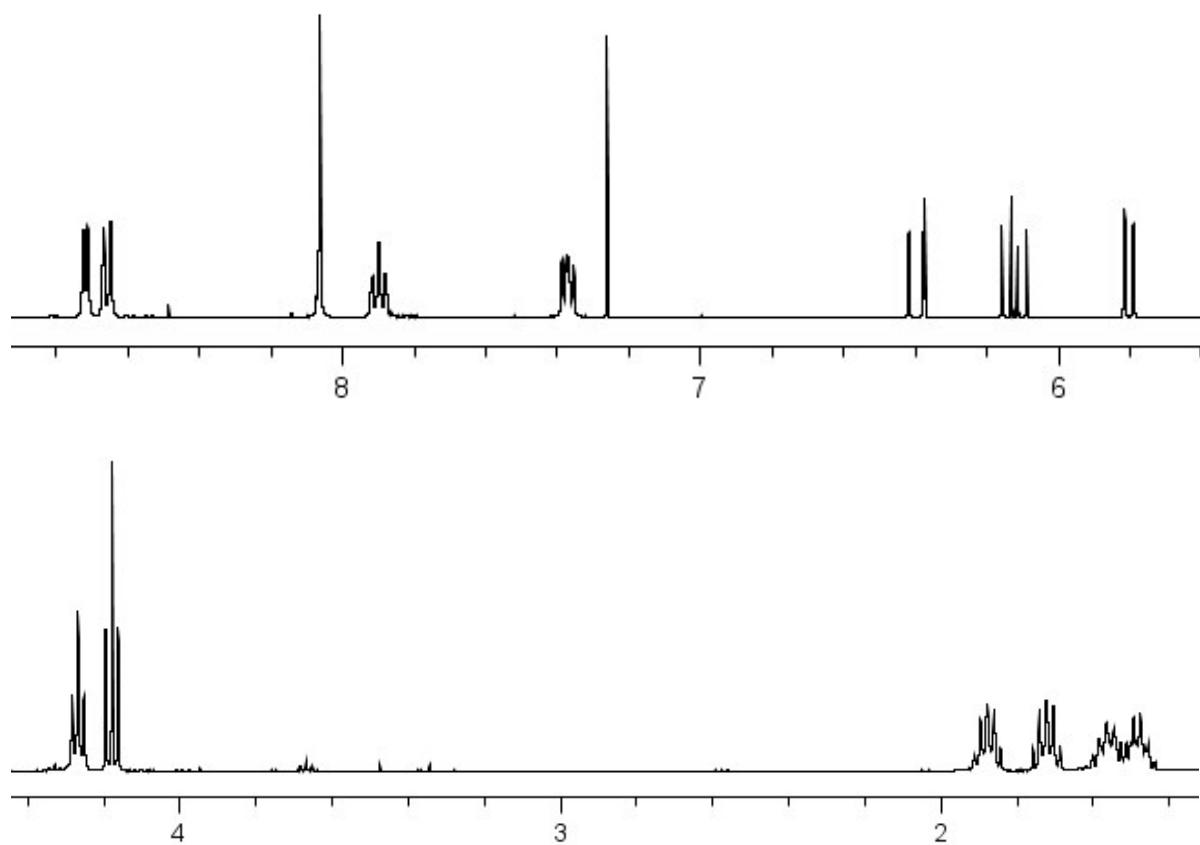


**Figure S-2a.** Regions of interest of  $^1\text{H}$  NMR spectra of TP monomer (in  $\text{CDCl}_3$ )

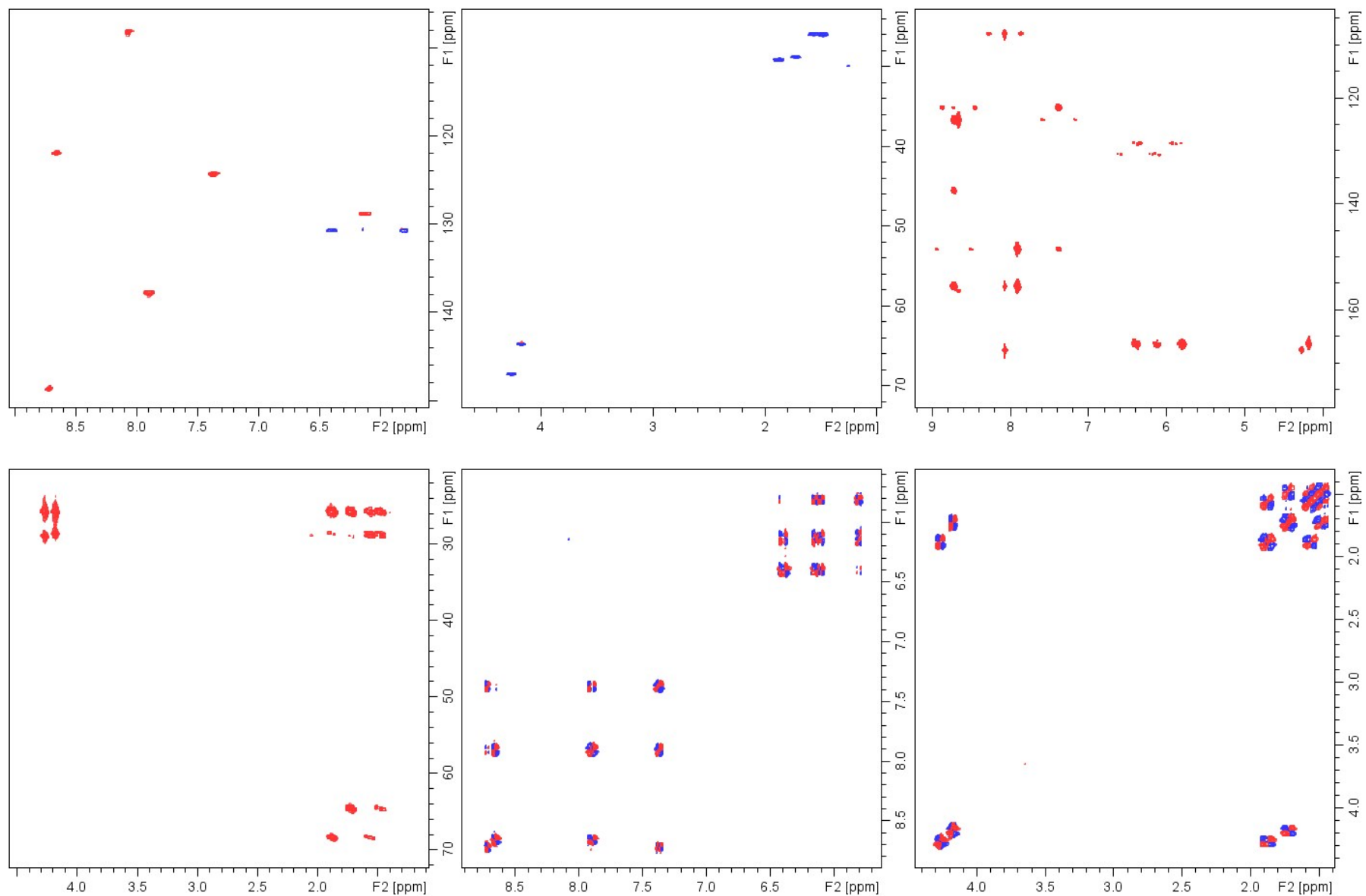


**Figure S-2b.** Regions of interest of  $^1\text{H}$ - $^{13}\text{C}$  HSQC, HMBC and  $^1\text{H}$ - $^1\text{H}$  DQF-COSY NMR spectra of TP monomer (in  $\text{CDCl}_3$ )

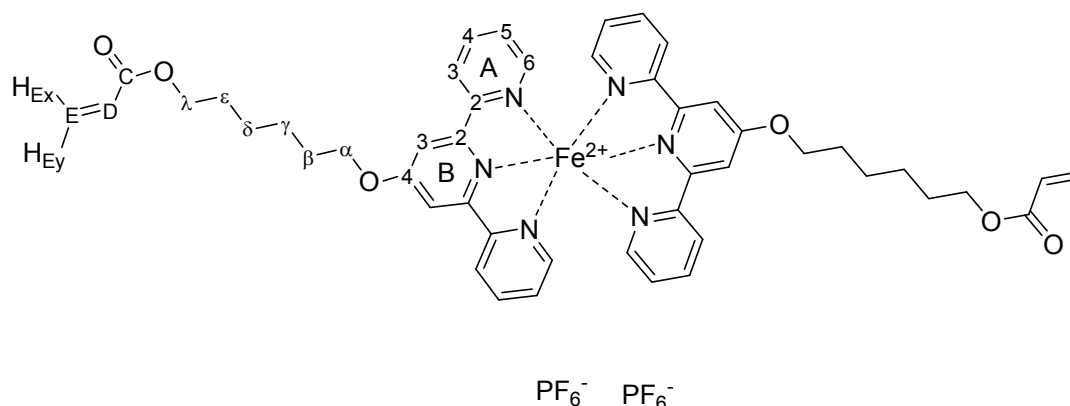


## Characterization of TP1 complexes with Fe(II) and Co(II)

### Synthesis and characterization of TP1/ Fe(II) complex

Ligand TP1 (69.8 mg, 0.173 mmol) and iron(II) chloride (11 mg, 0.0865 mmol) were added together in a ratio of 2:1 (ligand/metal) in methanol (10 mL). The reaction mixture changed to dark purple immediately and was stirred for 30 minutes. The solution was treated with excess ammonium hexafluorophosphate and water (3 mL) to precipitate  $[\text{Fe}(\text{TP1})_2][\text{PF}_6]_2$  as a purple solid. The suspension was filtered over Celite and washed with water, ethanol and diethyl ether to remove impurities. The pure purple product was washed off Celite with acetonitrile and dried under vacuum.

Yield: 62 mg, 0.072 mmol, 83%.



**Scheme S-3.** Chemical structure of TP1 complex with Fe(II) with labelled positions used for assignments of  $^1\text{H}$  and  $^{13}\text{C}$  NMR data.

$^1\text{H}$ -NMR (500 MHz,  $\text{CD}_3\text{CN}$ ,  $25^\circ\text{C}$ )  $\delta$ : 8.46 (s, 4H,  $\text{H}_{\text{B}3}$ ), 8.44 (m, 4H,  $\text{H}_{\text{A}3}$ ), 7.88 (m, 4H,  $\text{H}_{\text{A}4}$ ), 7.16 (m, 4H,  $\text{H}_{\text{A}6}$ ), 7.09 (m, 4H,  $\text{H}_{\text{A}5}$ ), 6.39 (dd, 2H,  $J = 17.4$  and  $1.5$  Hz,  $\text{H}_{\text{E}y}$ ), 6.20 (dd, 2H,  $J = 17.4$  and  $10.5$  Hz,  $\text{H}_{\text{D}}$ ), 5.88 (dd, 2H,  $J = 10.5$  and  $1.5$  Hz,  $\text{H}_{\text{E}x}$ ), 4.63 (t, 4H,  $J = 6.5$  Hz,  $\text{H}_{\alpha}$ ), 4.26 (t, 4H,  $J = 6.7$  Hz,  $\text{H}_{\lambda}$ ), 2.11 (m, 4H,  $\text{H}_{\beta}$ ), 1.83 (m, 4H,  $\text{H}_{\epsilon}$ ), 1.74 (m, 4H,  $\text{H}_{\gamma}$ ), 1.63 (m, 4H,  $\text{H}_{\delta}$ ).

$^{13}\text{C}\{^1\text{H}\}$ -NMR (126 MHz,  $\text{CD}_3\text{CN}$ ,  $25^\circ\text{C}$ )  $\delta$ : 168.0 ( $\text{C}_{\text{B4}}$ ), 166.0 ( $\text{C}_{\text{C}}$ ), 160.8 ( $\text{C}_{\text{B2}}$ ), 158.1 ( $\text{C}_{\text{A2}}$ ), 153.3 ( $\text{C}_{\text{A6}}$ ), 138.4 ( $\text{C}_{\text{A4}}$ ), 130.3 ( $\text{C}_{\text{E}}$ ), 128.6 ( $\text{C}_{\text{D}}$ ), 127.1 ( $\text{C}_{\text{A5}}$ ), 123.5 ( $\text{C}_{\text{A3}}$ ), 111.3 ( $\text{C}_{\text{B3}}$ ), 70.5 ( $\text{C}_{\alpha}$ ), 64.3 ( $\text{C}_{\lambda}$ ), 28.5 ( $\text{C}_{\beta}$ ), 28.3 ( $\text{C}_{\epsilon}$ ), 25.4 ( $\text{C}_{\delta}$ ), 25.3 ( $\text{C}_{\gamma}$ ).

Elemental Analysis: Calculated for  $\text{C}_{48}\text{H}_{50}\text{F}_{12}\text{FeN}_6\text{O}_6\text{P}_2$ : C, 50.01; H, 4.37; N, 7.29. Found: C, 49.83; H, 4.86; N, 7.45.

ESI-MS:  $m/z$  431.3 m.u.  $[\text{M}-2\text{PF}_6]^{2+}$  (calc. 431.3 m.u.).

### TP1/Co(II) complex characterization

In Fig. S-3a – S-3c regions of interest of the  $^1\text{H}$ ,  $^1\text{H}$ - $^{13}\text{C}$  HSQC and  $^1\text{H}$ - $^1\text{H}$  DQF-COSY NMR spectra of the paramagnetic Co(II)/TP1 complex are shown. Exceptionally large and unusual  $^1\text{H}$  and  $^{13}\text{C}$  NMR chemical shift values of up to 110 and 490 ppm, respectively, were determined for the Co(II) complex. Unfortunately, the full chemical shift assignment of the Co(II)/TP1 complex is not really trivial, since owing to the considerably broad  $^1\text{H}$  NMR signals the recoding of e.g.  $^1\text{H}$ - $^{13}\text{C}$  long range correlation experiments completely failed. Nevertheless, the assignment of  $^1\text{H}$  &  $^{13}\text{C}$  chemical shifts was possible i) over a walk through the DQF-COSY spectra (see Fig S-3c) from Position 1 (signal at 15.1 ppm) to 6 of the side chain (S) and ii) from the corresponding cross peaks in the HSQC spectrum the  $^{13}\text{C}$  chemical shifts were evaluated (Fig. S-3b). The assignment of the terpyridine moiety next to the paramagnetic center was much more difficult since the excitation and as well, the inversion of magnetization in the 2D NMR pulse sequences of that wide region in the  $^1\text{H}$  and  $^{13}\text{C}$  dimensions is a prerequisite. The connectivity of H-3A, H-4A and H-5A was monitored by correlations of the resonance at 6.62 ppm to protons at 69.4 and 33.9 ppm (Fig. S-3c). From chemical shift reasons, the  $\approx$  250 Hz broad resonance at 109 ppm was assigned to H-6A and the remaining signal at 73.7 ppm must belong to H-3A. This  $^1\text{H}$  NMR chemical shift assignments perfectly matches the data given by E.C. Constable et al.<sup>4</sup> for a Co(II) complex with a TP ligand substituted by a methoxy group at the B4 position. The  $^1\text{H}$ - $^{13}\text{C}$  HSQC NMR spectra (see Fig. S-3b) both were recorded without multiplicity editing and omitting shaped pulses to enable the excitation of the biggest possible spectral regions. By varying the widths and the carrier frequencies in the  $^{13}\text{C}$  dimension the unusually high  $^{13}\text{C}$  chemical shifts of 493.0 (C-65), 370.4 (C-3B) and 346.4 (C-A3) were unambiguously assigned. These values are in very good agreement with the data given for a similar

compound (Co(II)-complex of ligand 9 (p. 149)<sup>5</sup>, which to our knowledge was not published so far. In this work, the <sup>13</sup>C chemical shifts were assigned over selectively proton decoupled 1D <sup>13</sup>C NMR experiments. It must be mentioned that in our case the recording of 1D <sup>13</sup>C NMR experiments was not possible, since higher concentrated NMR solutions tended to spontaneous polymerization due to the presence of the terminal acrylate group. Due to the large line width, we did not observe a correlation of H-6A to any carbon in the HSQC NMR experiment and it is clear that we were not able to determine the <sup>13</sup>C chemical shift data for all quaternary carbons as well.

<sup>1</sup>H NMR (MeOD, 400.1 MHz):  $\delta$  108.9 (s (br), 2H, H-A6); 73.7 (s (br), 2H, H-B3); 69.4 (s (br), 2H, H-A3); 33.9 (s (br), 2H, H-A5); 15.1 (m (br), 2H, H-S1); 7.51 (m (br), 2H, H-S2); 7.05 (dd,  $J = 17.4+2.5$ , 1H, H-S9a); 6.98 (dd,  $J = 17.4+9.6$ , 1H, H-S8); 6.62 (s (br), 2H, H-A4); 6.35 (m (br), 2H, H-S3); 6.28 (dd,  $J = 9.6+2.5$ , 1H, H-S9b); 5.98 (t,  $J = 6.5$ , 2H, H-S6); 4.74 (m, 2H, H-S4); 4.11 (m, 2H, H-S5).

<sup>13</sup>C NMR (MeOD, 100.6 MHz):  $\delta$  493 (d, C-A5); 370.4 (d, C-B3); 346.4 (d, C-A3); 160.6 (d, C-A4); 132.0 (t, C-S9); 130.5 (d, C-S8); 80.9 (t, C-S1); 67.4 (t, C-S6); 38.5 (t, C-S2); 32.1 (t, C-S5); 31.3 (t, C-S3); 30.0 (t, C-S4).

<sup>1</sup>H-<sup>1</sup>H DQF-COSY correlations: H-A3  $\rightarrow$  H-(A4); H-A4  $\rightarrow$  H-(A3, A5); H-A5  $\rightarrow$  H-(A4); H-S1  $\rightarrow$  H-(S2); H-S2  $\rightarrow$  H-(S1, S3); H-S3  $\rightarrow$  H-(S2, S4); H-S4  $\rightarrow$  H-(S3, S5); H-S5  $\rightarrow$  H-(S4, S6); H-S6  $\rightarrow$  H-(S5); H-S8  $\rightarrow$  H-(S9a, S9b); H-S9a  $\rightarrow$  H-(S8, S9b); H-S9b  $\rightarrow$  H-(S8, S9a).

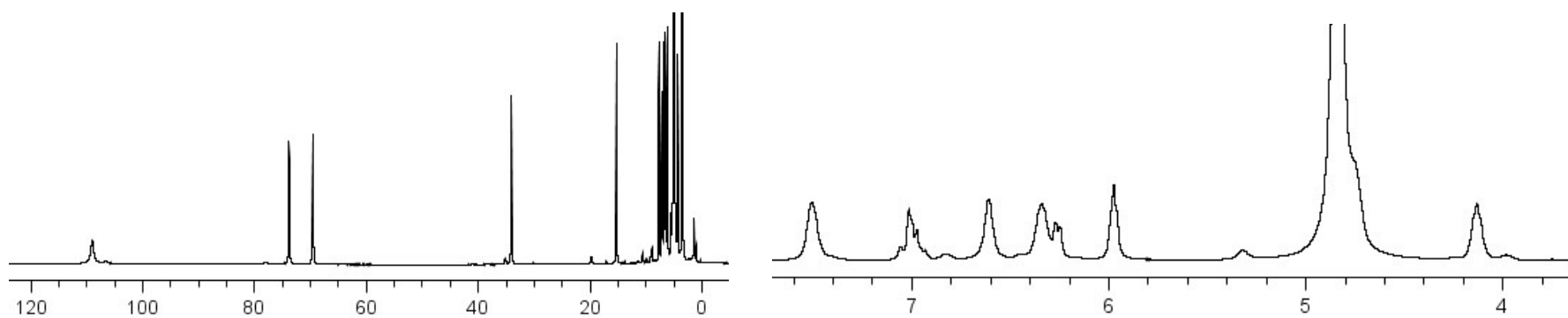


**Figure S-3a.** Full and enlarged region of  $^1\text{H}$  NMR spectrum of paramagnetic TP1/Co(II) (in  $\text{CD}_3\text{OD}$ )

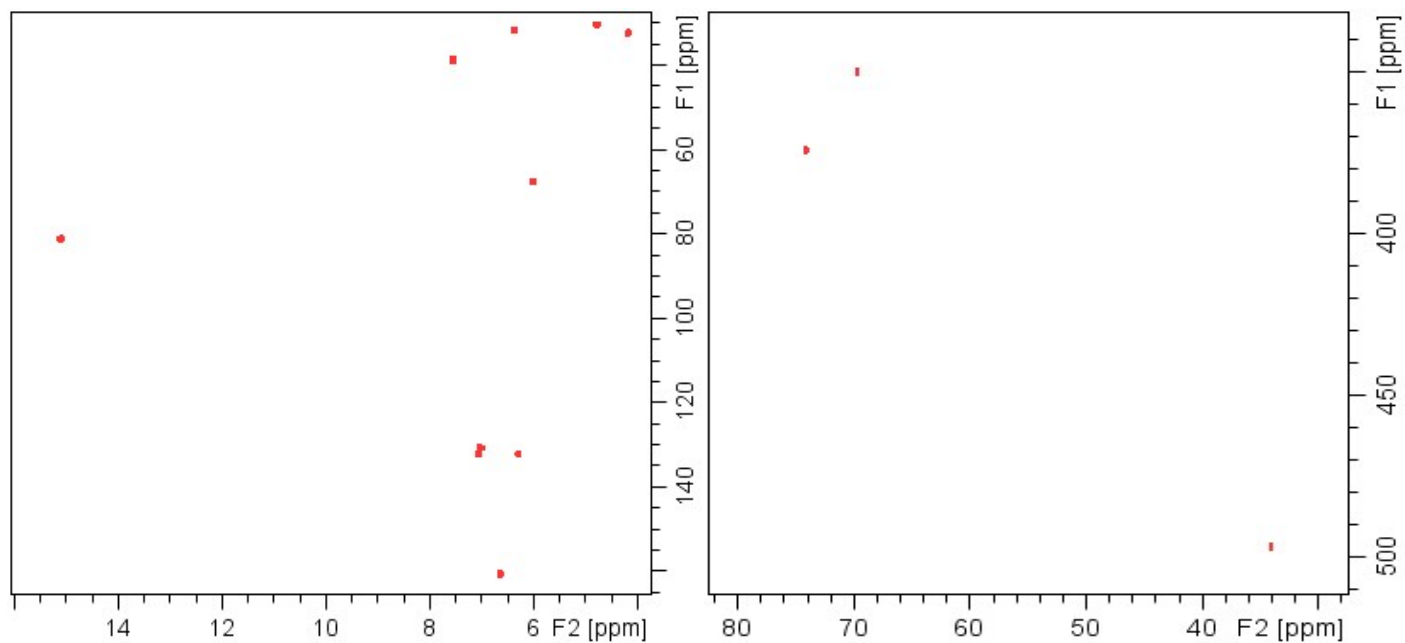


**Figure S-3b.** Regions of interest of  $^1\text{H}$ - $^{13}\text{C}$  HSQC NMR spectrum of paramagnetic TP1/Co(II) (in  $\text{CD}_3\text{OD}$ )

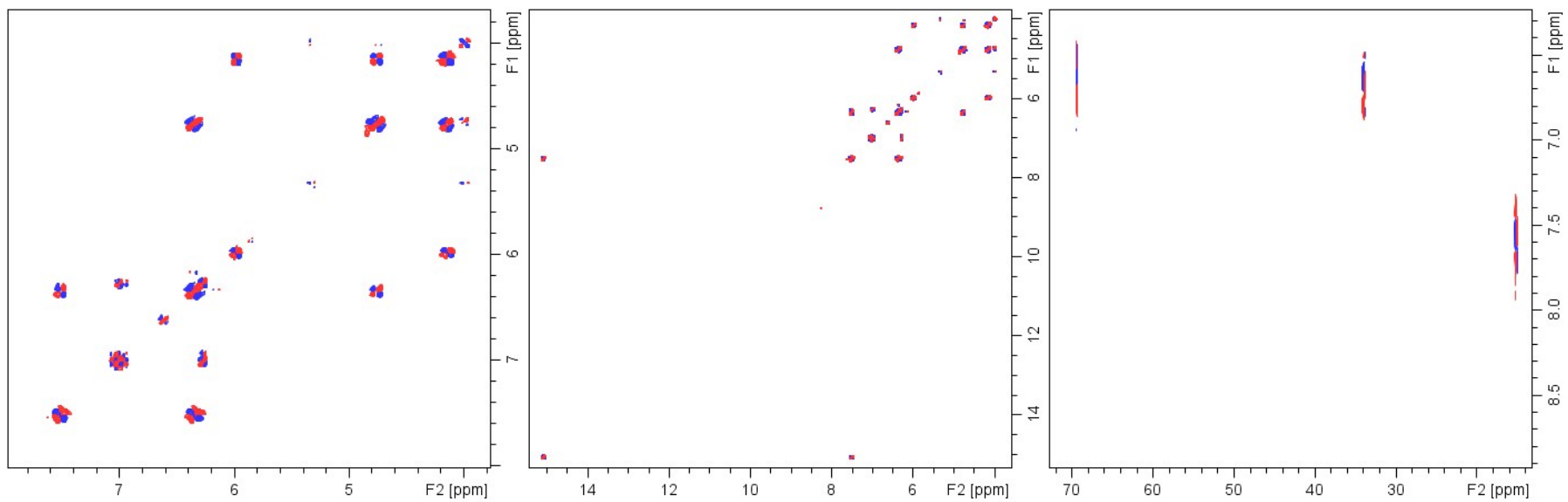


**Figure S-3c.** Regions of interest of  $^1\text{H}$ - $^1\text{H}$  DQF-COSY NMR spectra of paramagnetic TP1/Co(II) (in  $\text{CD}_3\text{OD}$ )

## Characterization of amphiphilic co-networks (APCNs) functionalized with TP1

### Quantification of TP1 inside the membranes

Four membranes with TP1 (10.3 mg, 0.026 mmol) were synthesized according to the method given in the experimental section and immersed for 12 h in 45 ml of a THF/water 50/50 vol-% solution. Then, 2.5 ml of this solution were analyzed by UV-Vis in a cuvette while stirring at 30°C. The amount of TP1 inside the solution was calibrated by adding progressively 5  $\mu$ l, then 10  $\mu$ l of a 0.1 g/l  $\text{FeCl}_2 \cdot 4\text{H}_2\text{O}$  aqueous solution. After each addition, the solution was stirred for 2 min and the absorbance at 556 nm was registered with a Varian 50Bio/50MPR system. The intersection of the two tangents at the beginning and the end of the curve gives an equivalence point at  $4.0 \cdot 10^{-5}$  mmol of  $\text{FeCl}_2 \cdot 4\text{H}_2\text{O}$  corresponding to 5.64% of the total mass of TP1 that did not polymerize.

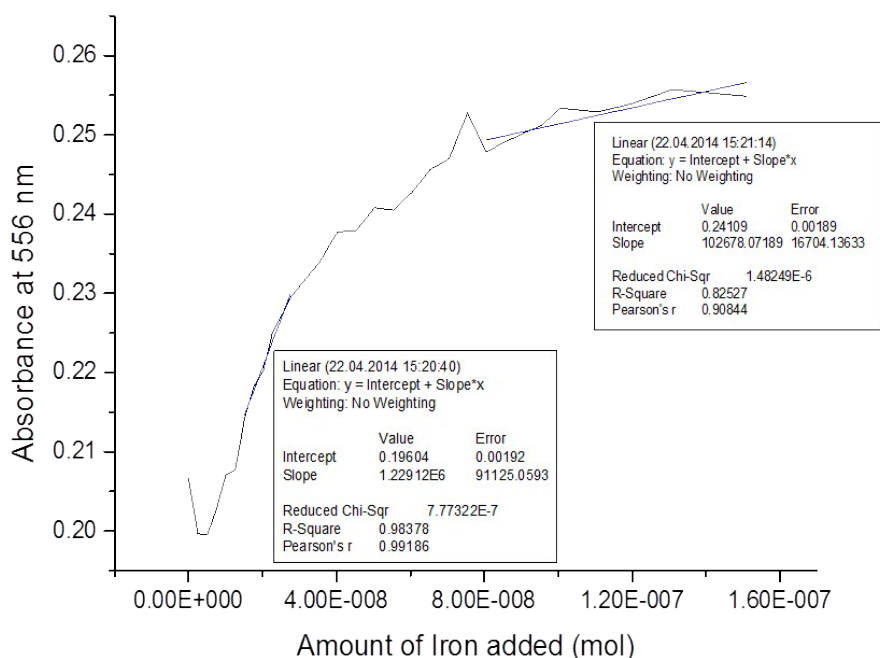


**Figure S-4.** Absorbance at 556 nm vs. Fe(II) concentration used for the quantification of TP1 covalently attached to the membrane.

### Volumetric degree of swelling measurement

All dimensions were determined with a Mitutoyo 522 Diamond Master Vernier. A membrane was dried in the desiccator over molecular sieves for one day. Afterwards, its volume ( $V_0$ ) was determined by measuring the side lengths and the thickness. Then the membrane was placed into water or hexane for 24 h and the volume ( $V_1$ ) was measured again. Each measurement was repeated three times. The volumetric degree of swelling  $S$  was calculated using the following formula:

$$S = \frac{V_1}{V_0} \quad [1]$$

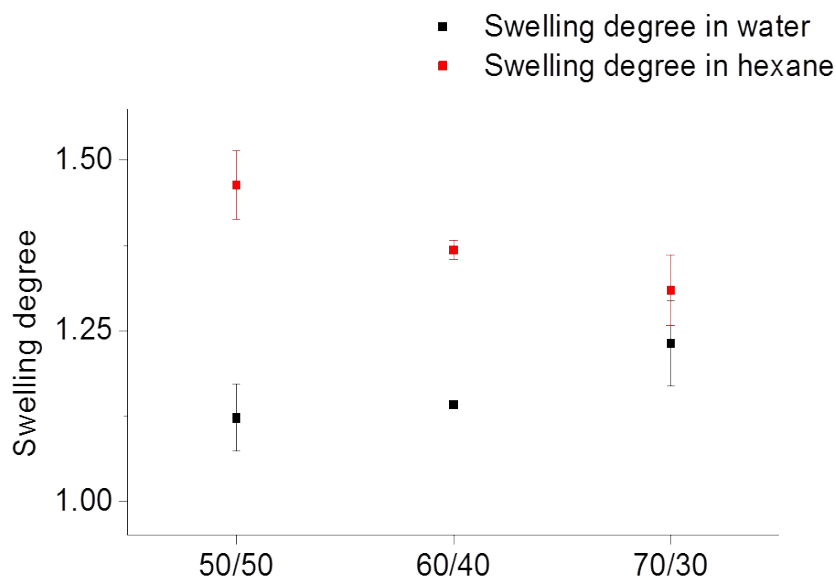


**Figure S-5.** Swelling degree of APCNs in water and hexane at different ratio between 2-((trimethylsilyl)oxy)ethyl acrylate (TMS-HEA) and  $\alpha,\omega$ -methacryloxypropyl poly(dimethylsiloxane) (PDMS-DMA) all of them functionalized with 0.4 wt.-% of TP1.

### Influence of TP1 on permeability and degree of swelling

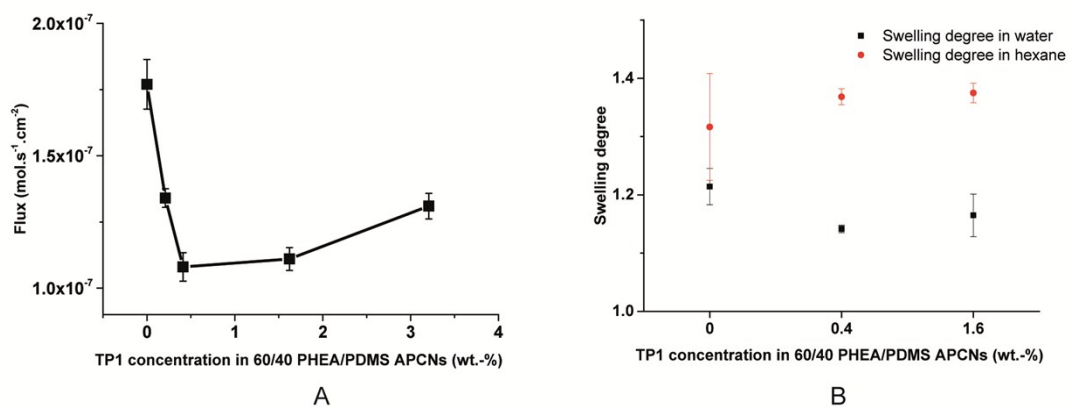


**Figure S-6.** Variation of permeability of caffeine (A) and swelling degree (B) of APCNs membrane at TMS-HEA/PDMS ratio of 60/40 functionalized with different amounts of TP1.

### XPS measurements

XPS measurements (PHI 5600 spectrometer) were done using non-monochromatized Mg-K $\alpha$  radiation (1253.6 eV) and operated at 300 W. The operating pressure of the XPS analysis chamber was approximately 1.10<sup>-8</sup> Torr. The spectra were collected at photoemission angles of 45° with respect to the surface normal. The relative sensitivity factors of 0.314 for C1s, 0.733 for O1s, 0.368 Si2p, 0.499 N1s and 1.964 for Fe2p<sub>3/2</sub> have been used for quantification.

**Table S-1.** XPS analysis of APCNs membrane (60/40 TM-HEA/PDMS) with 1.6 wt-% TP1

Name	Bonds	Position (eV)	Area	% Conc. found	% Conc. theory
C 1s	C-C, C-H	284.99	4881.2	40.02	40.39
C 1s	C-C, C=C	286.11	1517.5	12.44	13.66
C 1s	C=O	289.06	210.0	1.72	6.24
O 1s	/	533.08	6817.4	23.94	28.84
Si 2p	Si-O	102.29	3060.5	21.41	10.63
N 1s	N in organic matrix	400.44	89.78	0.46	0.24



## Characterization of APCNs functionalized with TP1 and SP

### Optical properties

UV spectra were recorded with a Lambda 9 spectrometer (Perkin Elmer) in the transmission mode. The UV irradiation experiments were carried out with a UV-light source (intraLED UV Volpi, 386 nm, 1.5 mW.cm<sup>-2</sup>) or with the white light source intraLED 3 from Volpi (400-700 nm, 500 lumen). After illuminating the membrane for 1 min with white light, the spectrum of the membrane was measured between 200 and 800 nm. Subsequently, the membrane was illuminated for 1 min with UV light and the spectrum was measured again. Three APCN membranes with 0.4 wt-% of TP1 and 1.0 wt-% SP were analyzed: One uncomplexed, one complexed in CoCl<sub>2</sub> and one in FeCl<sub>2</sub>.

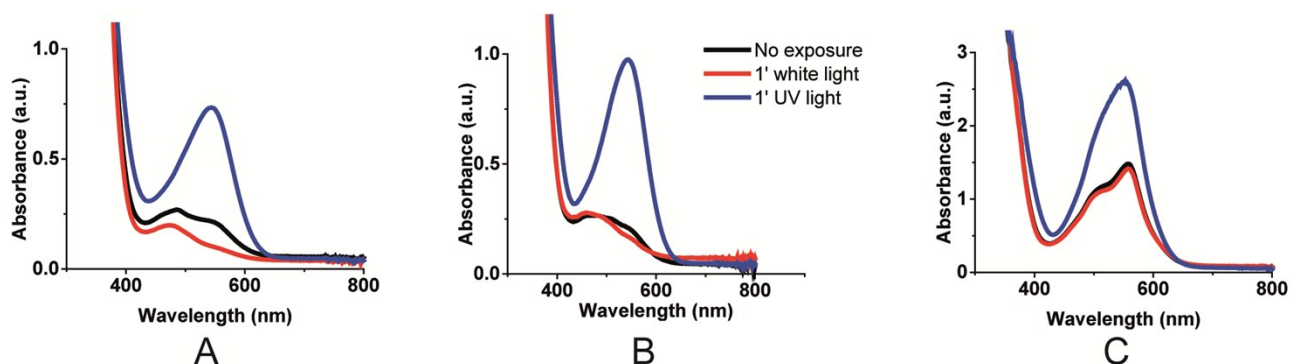
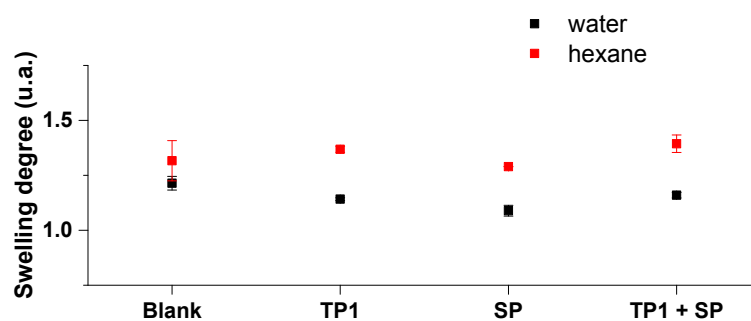


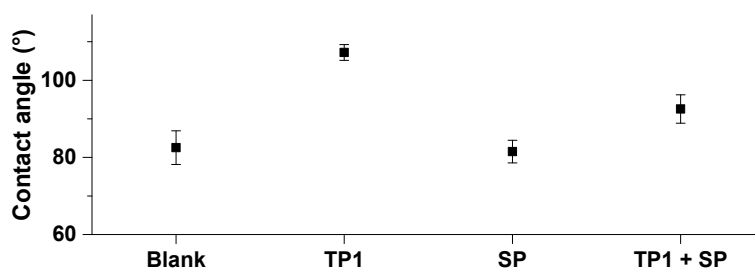
**Figure S-7.** UV-Vis profiles before and after light switch of spiropyran units (SP) for APCNs functionalized with 0.4 wt-% of TP1 and 1.0 wt-% of SP A) in the absence of metal ions, B) in presence of CoCl<sub>2</sub> and C) in the presence of FeCl<sub>2</sub>.

### Degree of swelling and contact angle:

Contact angles of the membranes were measured using a Krüss DSA25 device. They specimen were previously dried in a desiccator over molecular sieves for 18 h. The value given is an average over ten measured membranes.

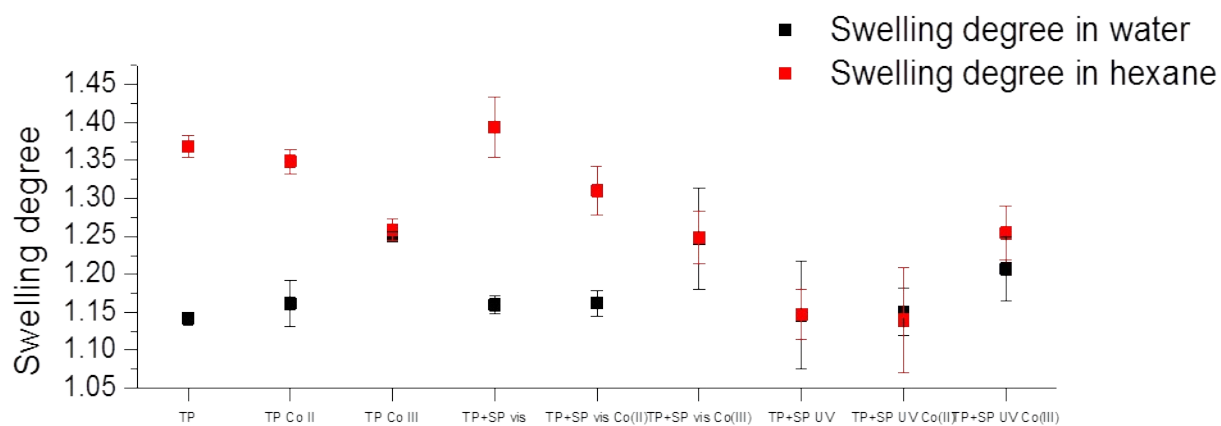


A

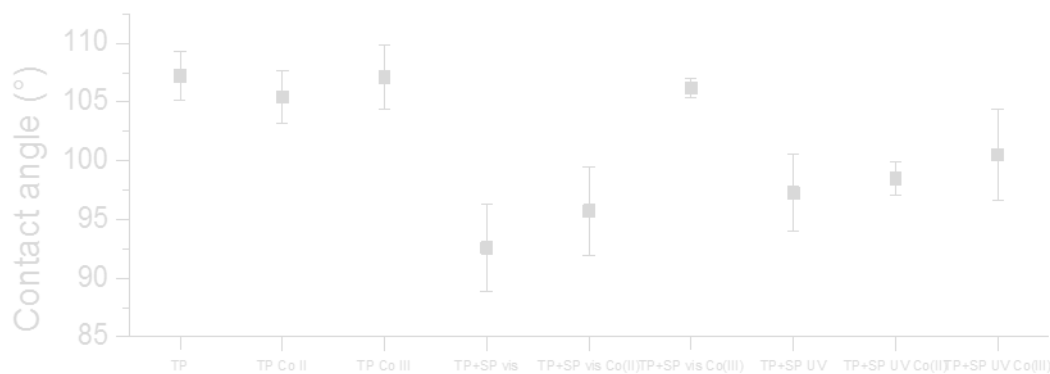


B

**Figure S-8.** A) Swelling degree in water (■) and hexane (■) and B) contact angle in water of APCNs membrane PHEA/PDMS 60/40 without any functionalization (blank), APCNs functionalized with 0.4 wt-% of TP1, APCNs functionalized with 1.0 wt-% SP only and APCNs functionalized with 0.4 wt-% of TP1 and 1.0 wt.-% of SP.



A



## B

**Figure S-9.** A) Swelling degree in water (■) and hexane (■) and B) contact angle in water of APCNs membranes PHEA/PDMS 60/40 functionalized with 0.4 wt-% of TP1 (TP in the Figure), complexed with Co(II) or Co(III) in the absence and in the presence of 1 wt-% of SP in the merocyanine form (SP vis) and in its spiropyran form (SP UV).

- 1 L. Baumann, D. de Courten, M. Wolf, R. M. Rossi and L. J. Scherer, *ACS Appl. Mater. Interfaces*, 2013, **5**, 5894–5897.
- 2 L. Baumann, K. Schöller, D. de Courten, D. Marti, M. Frenz, M. Wolf, R. M. Rossi and L. J. Scherer, *RSC Adv.*, 2013, **3**, 23317–23326.
- 3 S. Bode, L. Zedler, F. H. Schacher, B. Dietzek, M. Schmitt, J. Popp, M. D. Hager and U. S. Schubert, *Adv. Mater.*, 2013, **25**, 1634–8.
- 4 E. C. Constable, K. Harris, C. E. Housecroft, M. Neuburger and S. Schaffner, *Chem. Commun.*, 2008, 5360–2.
- 5 H. S. Chow, PhD thesis, 2005 URL: [edoc.unibas.ch/194/1/DissB\\_7029.pdf](http://edoc.unibas.ch/194/1/DissB_7029.pdf).